

Inverse Spin Hall Effect by Spin Injection

S. Y. Liu,^{1,*} Norman J. M. Horing,² and X. L. Lei¹

¹Department of Physics, Shanghai Jiaotong University, 1954 Huashan Road, Shanghai 200030, China

²Department of Physics and Engineering Physics, Stevens Institute of Technology, Hoboken, New Jersey 07030, USA

Motivated by a recent experiment [Nature **442**, 176 (2006)], we present a quantitative microscopic theory to investigate the inverse spin-Hall effect with spin injection into aluminum considering both intrinsic and extrinsic spin-orbit couplings using the orthogonalized-plane-wave method. Our theoretical results are in good agreement with the experimental data. It is also clear that the magnitude of the anomalous Hall resistivity is mainly due to contributions from extrinsic skew scattering, while its spatial variation is determined by the intrinsic spin-orbit coupling.

PACS numbers: 72.25.Ba, 72.25.Hg, 71.70.Ej

In the presence of an applied electric field, spin-orbit (SO) coupling can cause deflection of electrons with opposite spins in opposite directions, resulting in a nonvanishing transverse spin current. This so-called spin-Hall effect (SHE), which was first predicted by D'yakonov and Perel in 1971 [1] and was recently emphasized by Hirsch [2], has attracted a great deal of experimental and theoretical interest [3] because of its potential applications in Spintronics. Depending upon its origin, the SHE is classified into two types: intrinsic [1, 2, 4] and extrinsic SHE [5, 6]. Experimental observations of SHE have also been reported recently [7, 8, 9, 10].

The SO coupling mechanism can also lead to a reciprocal SHE effect, the "inverse spin-Hall effect" (ISHE), which was predicted by Hirsch [2]. When a purely longitudinal spin current is applied, the electrons with opposite spins, flowing in opposing longitudinal directions, move toward the same transverse side of the sample due to SO interaction, resulting in charge accumulation. Recently, Valenzuela and Tinkham presented a first clear ISHE observation [11]. By a nonlocal spin injection into metallic aluminum through a ferromagnetic/nonmagnetic contact (the configuration is illustrated in Fig. 1), they observed a finite Hall resistivity of order of milli-Ohms over a spin-diffusion length of the order of μm .

It is well known that spin [12] and charge [13] relaxations in aluminum are strongly influenced by band-structure anomalies which arise mainly from several accidental degeneracy points (near W points) in the Brillouin zone (BZ). Therefore, in an analysis of the ISHE by spin injection in aluminum, the momentum dependence of the scattering should be taken into account. Earlier work by Zhang analyzing the SHE in the presence of spin diffusion treated only momentum-independent relaxation [14]. In this Letter, we provide a realistic, quantitative theory for ISHE by spin injection in aluminum considering the momentum dependencies of the scattering rates and of the side-jump and skew scattering contributions to the anomalous Hall current (AHC). Both the intrinsic and extrinsic SO couplings are taken into account and the electronic bands and states are determined by

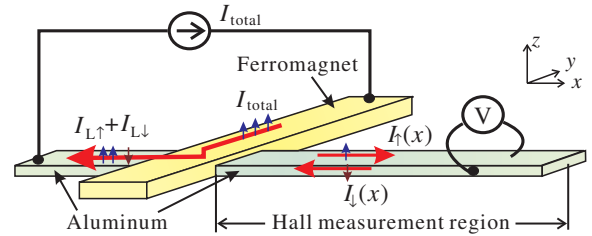


FIG. 1: (Color online) Measurement apparatus configuration for the spin injection experiment of Ref. [11]. A net current I_{total} is injected through aluminum (Al) via a ferromagnetic contact and it flows away from the Hall measurement region. Near the contact, *i.e.* at $x = 0$, $I_{\text{total}} = I_{L\uparrow} + I_{L\downarrow}$, $I_{L\downarrow} = I_{\downarrow}(x = 0)$, and $I_{\uparrow}(x = 0) + I_{\downarrow}(x = 0) = 0$, resulting in a vanishing net electric current for $x > 0$ and a finite spin current, $I_{\uparrow}(x) - I_{\downarrow}(x)$, over a distance of order of the spin-diffusion length.

the orthogonalized-plane-wave (OPW) method. The resulting Hall resistivities are in good agreement with the experimental data. It is also clear that, with spin injection into aluminum, the spatial variation of AHC is determined by the intrinsic SO coupling while its magnitude is mainly due to contributions from the extrinsic skew scattering.

In general, the SO interaction induced by ionic fields, *i.e.* the intrinsic SO coupling, may affect both the energy bands and the states of electrons in solids. However, in aluminum, its effect on the electronic band structure can be ignored. Hence, in our treatment, the energy band structure of electrons is determined by the standard OPW method in the absence of SO interaction, while the electronic Bloch states are a mixture of spin up and spin down species: $\psi_{n\mathbf{p}}^{(\mu)}(\mathbf{r}) = \sum_{\mathbf{G}} [a_{n\mathbf{p}}^{(\mu)}(\mathbf{G})|\mu\rangle + b_{n\mathbf{p}}^{(\mu)}(\mathbf{G})|\bar{\mu}\rangle] \exp[i(\mathbf{p} - \mathbf{G}) \cdot \mathbf{r}]$, with $\mu = 1, 2$ representing spinors ($\bar{\mu} = 3 - \mu$), \mathbf{p} as lattice momentum confined to the first BZ, n as band index, and \mathbf{G} as reciprocal lattice vector. The coefficient $a_{n\mathbf{p}}^{(\mu)}(\mathbf{G})$ is de-

terminated by the pseudopotential form of the Schrödinger equation, while $b_{n\mathbf{p}}^{(\mu)}(\mathbf{G})$ is obtained from first-order perturbation theory by taking account of the SO part of the pseudopotential, $\lambda \tilde{\mathbf{L}} \cdot \tilde{\mathbf{S}} \mathcal{P}_1$ (λ is the SO coupling constant and \mathcal{P}_1 is the operator projecting on the orbital angular momentum state $l = 1$).

In the spirit of the pseudopotential method, the electron-impurity scattering potential, $V(\mathbf{p}, \mathbf{k})$, corresponding to scattering of an electron from state \mathbf{p} to state \mathbf{k} , is the difference between the impurity- and host-atom form factors with a structure factor correction for lattice distortion around the substitutional impurities. It involves not only a spin-independent part $V_0(\mathbf{p}, \mathbf{k})$ but also a SO part $V_{\text{SO}}(\mathbf{p}, \mathbf{k})$: $V(\mathbf{p}, \mathbf{k}) = V_0(\mathbf{p}, \mathbf{k}) + V_{\text{SO}}(\mathbf{p}, \mathbf{k})$. In general, the elements of $V_{\text{SO}}(\mathbf{p}, \mathbf{k})$, $V_{\text{SO}}^{\mu\nu}(\mathbf{p}, \mathbf{k})$, take the form, $V_{\text{SO}}^{\mu\nu}(\mathbf{p}, \mathbf{k}) \equiv A(p, k) \mathbf{p} \times \mathbf{k} \cdot \langle \nu | \vec{\sigma} | \mu \rangle$ with $\vec{\sigma}$ as the Pauli matrices, and $A(p, k)$ depending only on the magnitudes of the electron momenta \mathbf{p} and \mathbf{k} .

In the presence of spin diffusion, the transport properties of solids may be described by a Wigner distribution function $\hat{\rho}(n, \mathbf{p}, \mathbf{R})$, which is a 2×2 diagonal matrix depending on the band index n , and on both Wigner coordinates: microscopic electron momentum \mathbf{p} and macroscopic space coordinate $\mathbf{R} \equiv (x, y, z)$. Under steady state conditions, $\hat{\rho}(n, \mathbf{p}, \mathbf{R})$ obeys a kinetic (Boltzmann) equation given by

$$\begin{aligned} \frac{\mathbf{p}}{m} \cdot \nabla_{\mathbf{R}} \hat{\rho}_{\mu\mu}(n, \mathbf{p}, \mathbf{R}) &= \sum_{\mathbf{p}, \mathbf{k}, n'} \left\{ W_{\mu\mu}^{nn'}(\mathbf{p}, \mathbf{k}) \right. \\ &\quad \times [\hat{\rho}_{\mu\mu}(n', \mathbf{k}, \mathbf{R}) - \hat{\rho}_{\mu\mu}(n, \mathbf{p}, \mathbf{R})] \\ &\quad \left. + W_{\mu\bar{\mu}}^{nn'}(\mathbf{p}, \mathbf{k}) [\hat{\rho}_{\bar{\mu}\bar{\mu}}(n', \mathbf{k}, \mathbf{R}) - \hat{\rho}_{\mu\mu}(n, \mathbf{p}, \mathbf{R})] \right\}. \end{aligned} \quad (1)$$

Here, $W_{\mu\mu}^{nn'}(\mathbf{p}, \mathbf{k})$ and $W_{\mu\bar{\mu}}^{nn'}(\mathbf{p}, \mathbf{k})$, respectively, are the non-spin-flip and spin-flip scattering rates. They can be obtained by analyzing the matrix elements of the scattering potential:

$$\begin{aligned} W_{\mu\mu}^{nn'}(\mathbf{p}, \mathbf{k}) &= 2\pi\delta(\varepsilon_{n\mathbf{p}} - \varepsilon_{n'\mathbf{k}}) \\ &\times \left| \sum_{\mathbf{G}, \mathbf{G}'} \left\{ \left[a_{n'\mathbf{k}}^{(\mu)}(\mathbf{G}') + b_{n'\mathbf{k}}^{(\bar{\mu})}(\mathbf{G}') \right]^* \right. \right. \\ &\quad \times \left[a_{n\mathbf{p}}^{(\mu)}(\mathbf{G}) + b_{n\mathbf{p}}^{(\bar{\mu})}(\mathbf{G}) \right] V_0(\mathbf{p} - \mathbf{G}, \mathbf{k} - \mathbf{G}') \\ &\quad \left. \left. + [a_{n'\mathbf{k}}^{(\mu)}(\mathbf{G}')]^* a_{n\mathbf{p}}^{(\mu)}(\mathbf{G}) V_{\text{SO}}^{\mu\mu}(\mathbf{p} - \mathbf{G}, \mathbf{k} - \mathbf{G}') \right\} \right|^2 \end{aligned} \quad (2)$$

and

$$\begin{aligned} W_{\mu\bar{\mu}}^{nn'}(\mathbf{p}, \mathbf{k}) &= 2\pi\delta(\varepsilon_{n\mathbf{p}} - \varepsilon_{n'\mathbf{k}}) \\ &\times \left| \sum_{\mathbf{G}, \mathbf{G}'} \left\{ \left(a_{n\mathbf{p}}^{(\mu)}(\mathbf{G}) [b_{n'\mathbf{k}}^{(\bar{\mu})}(\mathbf{G}')]^* \right. \right. \right. \\ &\quad \left. \left. + b_{n\mathbf{p}}^{(\mu)}(\mathbf{G}) [a_{n'\mathbf{k}}^{(\bar{\mu})}(\mathbf{G}')]^* \right) V_0(\mathbf{p} - \mathbf{G}, \mathbf{k} - \mathbf{G}') \right. \\ &\quad \left. \left. + a_{n\mathbf{p}}^{(\mu)}(\mathbf{G}) [a_{n'\mathbf{k}}^{(\bar{\mu})}(\mathbf{G}')]^* V_{\text{SO}}^{\mu\bar{\mu}}(\mathbf{p} - \mathbf{G}, \mathbf{k} - \mathbf{G}') \right\} \right|^2, \end{aligned} \quad (3)$$

with $\varepsilon_{n\mathbf{p}}$ as the energy dispersion relation for n -th band electrons. Note that in Eqs. (2) and (3) both the intrinsic and extrinsic SO couplings are involved. The last term on the right-hand side of Eq. (1) leads to an exchange of electrons with different spins, causing spin relaxation. This so-called Elliot-Yafet spin-relaxation mechanism[15, 16] in aluminum has been carefully investigated by Fabian and Das Sarma taking account of electron-phonon scattering[12]. They found that spin relaxation in aluminum is determined mainly by several accidental degeneracy points near the W points in BZ.

It has already been demonstrated that intrinsic SO coupling can make a nonvanishing contribution to AHC if the off-diagonal elements of the distribution function are finite[17]. However, in the spin injection experiment, the distribution function is essentially diagonal since the off-diagonal driving forces, such as the electric field and Zeeman energy splitting, are negligible. In particular, in the experiment of Ref.[11], there is no external driving electric field in the Hall measurement region, while the Zeeman energy splitting for the maximum applied magnetic field, $B = 3.5\text{T}$, is only 0.2meV , much smaller than the free-electron Fermi energy of aluminum, $E_{\text{F}}^0 = 11.7\text{eV}$. Hence, to determine AHC, one only needs to consider the extrinsic SO coupling.

The extrinsic SO interaction makes nonvanishing contributions to AHC through two mechanisms: a side-jump process proposed by Berger[18] and also skew scattering given by Smit[19]. The side-jump AHC arises from a sidewise shift of the center of the electron wave packet, while the skew scattering contribution corresponds to an anisotropic enhancement of the wave packet due to electron-impurity scattering described in the second Born approximation[20]. Obviously, the analysis of spin injection in aluminum calls for the formulation of these two mechanisms of AHC in terms of a distribution function. In previous studies, these two AHC mechanisms were described in the framework of a momentum-independent relaxation time[21, 22], or in linear response theory[23], and hence the existing results can not be applied in the present study of the ISHE by spin injection in aluminum.

To analyze the side-jump process, we begin with the anomalous term of the current operator, which is associated with function $\langle \psi_{\mu}^+(\mathbf{r}_1, t) \psi_{\mu}(\mathbf{r}, t) \rangle$ ($\psi_{\mu}(\mathbf{r}, t)$ and $\psi_{\mu}^+(\mathbf{r}, t)$ are electron field annihilation and creation operators, respectively). Expanding the statistical average involved in this function to first order of the electron-impurity interaction and applying the Langreth algebra[24] taken jointly with the generalized Kadanoff-Baym ansatz[25, 26], we finally arrive at the form of the steady-state current, $\mathbf{J}^{\text{SJ}}(\mathbf{R})$, in the lowest-order gradi-

ent expansion of the Wigner coordinate \mathbf{R} :

$$J_{\alpha}^{\text{SJ}}(\mathbf{R}) = -i\pi e N_i \sum_{\substack{\mathbf{p}, \mathbf{q} \\ \mu, n, n'}} \sum_{\substack{\mathbf{G}_1, \mathbf{G}_2 \\ \mathbf{G}_3, \mathbf{G}_4}} (-1)^{\mu} \bar{A}^{(\mu)}(n\mathbf{p}, n'\mathbf{k}, \mathbf{G}_1, \mathbf{G}_2) \\ \times \bar{V}_0^{(\mu)}(n'\mathbf{k}, n\mathbf{p}, \mathbf{G}_3, \mathbf{G}_4) \varepsilon_{\alpha\beta z} [(\mathbf{k} - \mathbf{G}_2) - (\mathbf{p} - \mathbf{G}_1)]_{\beta} \\ \times \delta(\varepsilon_{n'\mathbf{k}} - \varepsilon_{n\mathbf{p}}) [\hat{\rho}_{\mu\mu}(n, \mathbf{p}, \mathbf{R}) - \hat{\rho}_{\mu\mu}(n', \mathbf{k}, \mathbf{R})], \quad (4)$$

with $\bar{A}^{(\mu)}(n\mathbf{p}, n'\mathbf{k}, \mathbf{G}_1, \mathbf{G}_2) \equiv [a_{n'\mathbf{k}}^{(\mu)}(\mathbf{G}_2)]^* a_{n\mathbf{p}}^{(\mu)}(\mathbf{G}_1) A(|\mathbf{p} - \mathbf{G}_1|, |\mathbf{k} - \mathbf{G}_2|)$, $\bar{V}_0^{(\mu)}(n\mathbf{p}, n'\mathbf{k}, \mathbf{G}_1, \mathbf{G}_2) \equiv [a_{n'\mathbf{k}}^{(\mu)}(\mathbf{G}_2)]^* a_{n\mathbf{p}}^{(\mu)}(\mathbf{G}_1) V_0(\mathbf{p} - \mathbf{G}_1, \mathbf{k} - \mathbf{G}_2)$, and $\varepsilon_{\alpha\beta z}$ as the totally antisymmetric tensor.

The skew scattering AHC, $\mathbf{J}^{\text{SS}}(\mathbf{R})$, is associated with the additional SO term of the distribution function in the second Born approximation. Substituting this term into the non-SO part of current operator, in the first order of SO coupling constant λ , $\mathbf{J}^{\text{SS}}(\mathbf{R})$ takes the form,

$$\mathbf{J}^{\text{SS}}(\mathbf{R}) = i4\pi^2 e N_i \sum_{\substack{\mathbf{p}, \mathbf{k}, \mathbf{q} \\ \mu, n, n', n''}} \sum_{\substack{\mathbf{G}_1, \mathbf{G}_2, \mathbf{G}_3 \\ \mathbf{G}_4, \mathbf{G}_5, \mathbf{G}_6}} \mathbf{v}_{n\mathbf{p}} \\ \times (-1)^{\mu} \delta(\varepsilon_{n'\mathbf{k}} - \varepsilon_{n\mathbf{p}}) \delta(\varepsilon_{n''\mathbf{q}} - \varepsilon_{n\mathbf{p}}) \\ \times \left\{ \bar{A}^{(\mu)}(n\mathbf{p}, n'\mathbf{k}, \mathbf{G}_1, \mathbf{G}_2) V_0^{(\mu)}(n'\mathbf{k}, n''\mathbf{q}, \mathbf{G}_3, \mathbf{G}_4) \right. \\ \left. \times V_0^{(\mu)}(n''\mathbf{q}, n\mathbf{p}, \mathbf{G}_5, \mathbf{G}_6) \varepsilon_{\alpha\beta z} [\mathbf{p} - \mathbf{G}_1]_{\alpha} [\mathbf{k} - \mathbf{G}_2]_{\beta} \right. \\ \left. + \left[\begin{array}{l} n\mathbf{p} \rightarrow n'\mathbf{k} \\ n'\mathbf{k} \rightarrow n''\mathbf{q} \\ n''\mathbf{q} \rightarrow n\mathbf{p} \end{array} \right] + \left[\begin{array}{l} n\mathbf{p} \rightarrow n''\mathbf{q} \\ n'\mathbf{k} \rightarrow n\mathbf{p} \\ n''\mathbf{q} \rightarrow n'\mathbf{k} \end{array} \right] \right\} \\ \times \hat{\rho}_{\mu\mu}(n', \mathbf{k}, \mathbf{R}) \tau(n', \mathbf{k}), \quad (5)$$

with $\mathbf{v}_{n\mathbf{p}} \equiv d\varepsilon_{n\mathbf{p}}/d\mathbf{p}$ as the electron velocity and N_i as the impurity density. $\tau(n', \mathbf{k})$ is the transport relaxation time, which has been carefully investigated in Ref. [13]. The last two terms in curly brackets of Eq. (5) are obtained from the first term by following the replacement rules indicated in the square brackets.

It should be noted that the side-jump and skew scattering contributions to AHC, $J_{\alpha}^{\text{SJ}}(\mathbf{R})$ and $J_{\alpha}^{\text{SS}}(\mathbf{R})$, exist in conjunction with a nonvanishing longitudinal spin current, rather than the net electric current. In a system with a longitudinal charge current but without magnetization, the electrons with opposite spins distribute equally and the factor $(-1)^{\mu}$ in Eqs. (4) and (5) leads to vanishing of the AHC. However, when a purely longitudinal spin current is present, we have $\hat{\rho}_{\mu\mu}^{(1)}(n', \mathbf{k}, \mathbf{R}) = -\hat{\rho}_{\bar{\mu}\bar{\mu}}^{(1)}(n', \mathbf{k}, \mathbf{R})$ with $\hat{\rho}^{(1)}(n', \mathbf{k}, \mathbf{R})$ as the deviation from the equilibrium Fermi distribution. Hence, the signs of contributions to Hall current from electrons having opposite spins are the same, resulting in a finite transverse charge current.

We perform a numerical calculation to investigate the ISHE in the spin injection experiment illustrated in Fig. 1. The electronic band structure of aluminum is evaluated by a *modified* 4 OPW method, in which

the 15 shortest reciprocal lattice vectors are considered but the pseudopotentials, except for Ashcroft's V_{111} and V_{200} [27], are assumed to vanish. This treatment enables us to obtain a continuous electron velocity when the electron momentum crosses from one symmetry section of the fcc BZ into another. The sums over all electron momenta in the first BZ are performed by the tetrahedron method[28]. Further, we assume that the electron-impurity interaction arises from defects, which may be introduced in the process of material fabrication. In this way, the scattering potential is just given by the form factor of aluminum but with the opposite sign. In the calculations, the spin-independent part of scattering potential is described by a screened Ashcroft form factor[29], while the SO part is chosen from Ref.[30] with SO coupling constant $\lambda = 2.4 \times 10^{-3}$ a.u.[12]. To determine the transverse Hall current, $J_y \equiv J_y^{\text{SJ}} + J_y^{\text{SS}}$, and the longitudinal spin current, $J_x^z(x) \equiv J_{\uparrow x}^z(x) - J_{\downarrow x}^z(x)$ with $J_{\mu x}(x) = \sum_{n, \mathbf{p}} e(\mathbf{v}_{n\mathbf{p}})_x \hat{\rho}_{\mu\mu}(\mathbf{p}, x)$, we solve the Boltzmann equation, Eq.(1), using the Fermi-surface-harmonic-expansion method[31], assuming an initial deviation from the equilibrium Fermi distribution, $\hat{\rho}_{\mu\mu}^{(1)}(n, \mathbf{p}, x = 0)$, of form: $\hat{\rho}_{\mu\mu}^{(1)}(n, \mathbf{p}, x = 0) = (-1)^{\mu} e \mathbf{E}_c \cdot \mathbf{v}_{n\mathbf{p}} \tau_{n\mathbf{p}} n'_{\text{F}}(\varepsilon_{n\mathbf{p}})$ with $n'_{\text{F}}(\varepsilon)$ as the derivative of the Fermi function. The effective electric field \mathbf{E}_c is obtained by considering the initial spin-up current densities injected into the right-hand side of the aluminum at $x = 0$ in the experiment of Ref. [11]: $J_{\uparrow x}(x = 0) = 3.75$ or 1.8×10^9 A/m² for samples with thicknesses $t = 12$ or 25 nm (in the experiment, $I_{\text{total}} = 50 \mu\text{A}$, the sample widths are $w = 400$ nm and the spin-polarization, $P \equiv (I_{L\uparrow} - I_{L\downarrow})/I_{\text{total}}$ at $x = 0$, is 0.28). The impurity densities are determined from the mobilities of the experimental samples.

In Fig. 2, we plot the longitudinal spin current J_x^z and the AHC J_y as functions of coordinate x for the two different values of $J_{\uparrow x}(x = 0)$. It is evident that with increasing x , $J_x^z(x)$ and $J_y(x)$ decrease exponentially: $J_x^z(x), J_y(x) \sim \exp(-x/x_{sd})$ with x_{sd} as the spin-diffusion length. For aluminum, we find $x_{sd}^{\text{theory}} = 830$ nm for $t = 25$ nm, and $x_{sd}^{\text{theory}} = 512$ nm for $t = 12$ nm, which are in good agreement with the experimental results: the experimental x_{sd} values are $x_{sd}^{\text{exp}} = 735$ nm for $t = 25$ nm and $x_{sd}^{\text{exp}} = 490$ nm for $t = 12$ nm.

From Fig. 2 we see that the AHC exists but is relatively small: it is almost five orders of magnitude smaller than $J_x^z(x)$. Nevertheless, the corresponding Hall voltage can be detected. We calculated the Hall resistivities for the two initial values of $J_{\uparrow x}(x)$ and compared them with the experimental data. The results are plotted in Fig. 3. Our theoretical results, without any adjustable parameters, are in good agreement with the data. For $t = 12$ nm (or $J_{\uparrow x}(0) = 3750$ A/m²), our theoretical values for R_{AHE} agree perfectly with the data. For $t = 25$ nm (or $J_{\uparrow x}(0) = 1800$ A/m²), the calculated re-

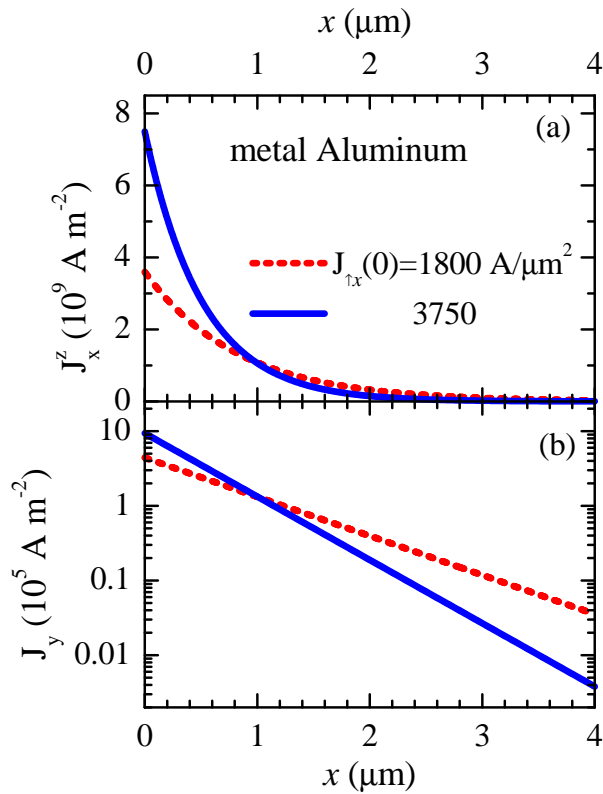


FIG. 2: (Color online) Coordinate dependencies of the longitudinal spin current, J_x^z (a), and anomalous Hall current, J_y (b), in the spin injection experiment for different initial values of $J_{\uparrow x}(x)$: $J_{\uparrow x}(0) = 3750$, and $1800 \text{ A}/\mu\text{m}^2$.

sults are a bit larger than those obtained experimentally. This may be due to the anisotropy of the experimental sample, which could lead to a different λ -value than the one we use here. Note that the sign of the calculated Hall voltage also agrees with that found experimentally: the positive spin current, $J_x^z(x)$, polarized along the positive z -direction produces a negative Hall electric field.

Our numerical calculation also shows that the contributions to AHC are dominated by skew scattering. The side-jump AHC contribution is only about 3.5% of the skew scattering one. This is due to the fact that the mobilities of the samples involved are small and the impurities are relatively dense: N_i is about 1% of the electron density. Note that the signs of both the side-jump and skew scattering AHC contributions are the same.

We also find that the effect of the extrinsic SO coupling on the diffusion length vanishes. This holds valid for materials with space inversion symmetry (SIS). In the case of weak SO coupling, $a_{n\mathbf{p}}^{(\mu)}$ is real: $a_{n\mathbf{p}}^{(\mu)} = [a_{n\mathbf{p}}^{(\mu)}]^*$, and SIS leads to $a_{n\mathbf{p}}^{(\bar{\mu})} \equiv a_{n,-\mathbf{p}}^{(\mu)} = a_{n\mathbf{p}}^{(\mu)}$. Hence, the extrinsic parts of the scattering rates are asymmetric under the momentum inversion operation, resulting in a vanishing contribution to the diffusion length. This implies that the spatial dependence of AHC is determined only by the

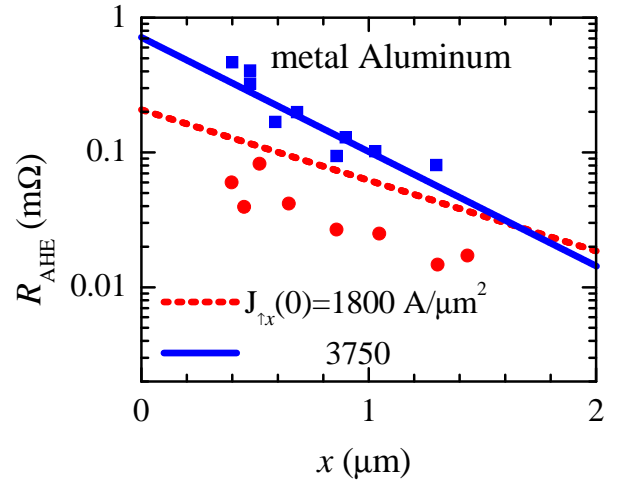


FIG. 3: (Color online) Anomalous Hall resistivities, R_{AHE} , as functions of coordinate x for different initial values of $J_{\uparrow x}(x)$: $J_{\uparrow x}(0) = 3750, 1800 \text{ A}/\mu\text{m}^2$. The solid and dotted lines are our theoretical results, and the squares (circles) are the experimental data for Al thicknesses $t = 12$ (25) nm (Ref. [11]).

intrinsic SO coupling since $J_{\alpha}^{\text{SJ}}(\mathbf{R})$ and $J_{\alpha}^{\text{SS}}(\mathbf{R})$ depend on \mathbf{R} only through the distribution function.

In conclusion, we have presented a fully microscopic theory to analyze the ISHE observed in the spin-injection experiment in aluminum taking account of both the intrinsic and extrinsic SO couplings. Employing the OPW method, the momentum-dependent scattering rates of the Boltzmann equation were treated carefully and the side-jump and skew scattering contributions to the AHC were formulated in terms of the distribution function. Performing realistic calculations for aluminum, we have determined anomalous Hall resistivities that are in good agreement with the experimental data.

The authors would like to thank Dr. S. O. Valenzuela for providing the details of their experiment and its setup. This work was supported by the Youth Scientific Research Startup Funds of SJTU, by projects of the National Science Foundation of China and the Shanghai Municipal Commission of Science and Technology, and by the Department of Defense through the DURINT program administered by the US Army Research Office, DAAD Grant No. 19-01-1-0592.

* Electronic address: liusy@mail.sjtu.edu.cn

- [1] M. I. Dyakonov and V. I. Perel, Phys. Lett. **35A**, 459 (1971).
- [2] J. E. Hirsch, Phys. Rev. Lett. **83**, 1834 (1999).
- [3] For a recent review, see J. Schliemann, Int. J. Mod. Phys. B, **20**, 1015 (2006).
- [4] H.-A. Engel, B. I. Halperin, and E. I. Rashba, Phys. Rev. Lett. **95**, 166605 (2005).

- [5] S. Murakami, N. Nagaosa, and S. C. Zhang, *Science* **301**, 1348 (2003).
- [6] J. Sinova, D. Culcer, Q. Niu, N. A. Sinitsyn, T. Jungwirth, and A. H. MacDonald, *Phys. Rev. Lett.* **92**, 126603 (2004).
- [7] Y. K. Kato, R. C. Myers, A. C. Gossard, D. D. Awschalom, *Science* **306**, 1910 (2004).
- [8] J. Wunderlich, B. Kaestner, J. Sinova, and T. Jungwirth, *Phys. Rev. Lett.* **94**, 047204 (2005).
- [9] H. Zhao, E. J. Loren, H. M. van Driel, and A. L. Smirl, *Phys. Rev. Lett.* **96**, 246601 (2006).
- [10] X.-D. Cui, S.-Q. Shen, J. Li, W. Ge, and F.-C. Zhang, cond-mat/0608546 (unpublished).
- [11] S. O. Valenzuela and M. Tinkham, *Nature* **442**, 176 (2006).
- [12] J. Fabian and S. Das Sarma, *Phys. Rev. Lett.* **81**, 5624 (1998); **83**, 1211 (1999).
- [13] R. S. Sorbello, *J. Phys. F: Metal Phys.* **4**, 1665 (1974).
- [14] S. Zhang, *Phys. Rev. Lett.* **85**, 393 (2000).
- [15] R. J. Elliott, *Phys. Rev.* **96**, 266 (1954).
- [16] Y. Yafet, in *Solid State Physics*, edited by F. Seitz and D. Turnbull (Academic, New York, 1963), Vol. 14.
- [17] S. Y. Liu and X. L. Lei, *Phys. Rev. B* **72**, 195329 (2005).
- [18] L. Berger, *Phys. Rev. B* **2**, 4559 (1970); **5**, 1862 (1972).
- [19] J. Smit, *Physica* **21**, 877 (1955); *ibid.* **24**, 39 (1958).
- [20] P. Leroux-Hugon and A. Ghazali, *J. Phys. C: Solid State Phys.* **5**, 1072(1972).
- [21] A. Crépieux and P. Bruno, *Phys. Rev. B* **64**, 014416 (2001); V. K. Dugaev, A. Crépieux, and P. Bruno, *ibid.* **64**, 104411(2001); A. Crépieux, J. Wunderlich, V. K. Dugaev, and P. Bruno, *J. Magn. Magn. Mater.* **242-245**, 464 (2002).
- [22] For a review, see J. Sinova, T. Jungwirth, and J. Černe, *Int. J. Mod. Phys. B* **18**, 1083 (2004).
- [23] S. Y. Liu, N. J. M. Horing, and X. L. Lei, *Phys. Rev. B* **74**, 165316 (2006).
- [24] H. Haug and A.-P. Jauho, *Quantum Kinetics in Transport and Optics of Semiconductors* (Springer, 1996).
- [25] P. Lipavský, V. Špička, and B. Velický, *Phys. Rev. B* **34**, 6933 (1986).
- [26] H. Haug, *Phys. Status Solidi (b)* **173**, 139 (1992).
- [27] N. W. Ashcroft, *Phil. Mag.* **8**, 2055 (1963).
- [28] A. H. MacDonald, S. H. Vosko, and P. T. Coleridge, *J. Phys. C* **12**, 2991 (1979).
- [29] M. Kaveh and N. Wiser, *Phys. Rev. B* **21**, 2291 (1980).
- [30] J. R. Anderson, W. J. O'Sullivan, and J. E. Schirber, *Phys. Rev. B* **5**, 4683 (1972).
- [31] P. B. Allen, *Phys. Rev. B* **13**, 1416 (1976).